

CHAPTER 47

Directional Growth for Numerical Wind Wave Models

W.L. Neu¹
S.H. Kwon²

Abstract

This study is concerned with the operation of spectral wind wave models. Many spectral wind wave models use a growth mechanism which operates on the point spectrum with directionality being introduced after the fact by the use of a spreading function. It is recognized here that this approach leads to errors whenever the wind and wave fields are not aligned. This is demonstrated by comparing the performance of two first generation models under various conditions. One makes use of a point spectral growth mechanism and follows the operation of the Spectral Ocean Wave Model (SOWM). The other uses a directional growth mechanism but is otherwise the same as the first. A large difference between the models is noted for swell corrupted seas.

1. Introduction

A number of operational wave forecasting models exist which perform with varying degrees of accuracy depending largely on the complexity of the situation they are asked to model. Since our understanding of the wave generation process is far from complete, wind wave models must rely heavily on empirical formulas. As long as the conditions a model is asked to simulate correspond with those under which the data for its empirical foundation were obtained, the model performs fairly well. When presented with situations of increased complexity, however, the performance of a model is bound to deteriorate. This was nicely illustrated in the Sea Wave Modeling Project (SWAMP Group, 1985).

In order to improve the performance of a wave model, it seems important to retain in the model as much detail and generality of the physics as possible. A large step in this direction was made by Pierson, et al. (1966) with the development of a model which computed directional wave spectra and allowed for the propagation of wave energy. After undergoing several refinements (Inoue, 1967; Lazanoff and Stevenson, 1975) it has evolved into the Spectral Ocean Wave Model (SOWM) as described by Pierson (1982). The SOWM is an operational wave model in use by the U.S. Navy Fleet Numerical Oceanography Center.

The SOWM is classified as a first generation decoupled propagation model in that the wave growth is dominated by wind energy input as

¹Assistant Professor, Virginia Polytechnic Institute and State University, Blacksburg, VA 24061, USA

²Lecturer, Pusan National University, Pusan, 607, Korea

opposed to nonlinear wave interaction effects and the spectrum is discretized into frequency-direction bands. Each band is allowed to evolve more or less independently and propagate at its own group velocity in its own direction. Other models of this type include those of Barnett (1968) and Ewing (1971).

Second generation discrete models, referred to as coupled discrete models rely heavily on nonlinear interactions in their growth mechanisms. These include the models of Resio (1981) and Golding (1983). The remaining class of models, the coupled hybrid models, are parametric models. These attempt to compute a set of parameters of a point spectrum, typically the JONSWAP spectrum (Hasselmann, et al., 1973), to represent the windsea part of the spectrum and require assumptions as to how the windsea becomes swell and vice versa. Thus they implicitly employ nonlinear energy transfer as the dominant mechanism controlling the spectral shape. An example is the model of Hasselmann, et al. (1976). Several models other than those referred to above and falling in all three classes are described by the SWAMP Group (1985).

The focus of this study is on the directional properties of the wave generation mechanism. By the design of the parametric models, the windsea part of the spectrum at least, must obtain its directionality from a spreading function centered on the wind direction. Some of these models allow the existence of swell whose direction of propagation is independent of the windsea, however, the directionality of any energy generated by the model must still be that of a spreading function.

The discrete models are not inherently so confined. Since they are discretized in direction, they may allow the directionality of the energy growth to be determined by the directionality of the growth mechanism. Further, since the growth rate of the spectrum is strongly dependent on sea state, the directionality (and, in general, magnitude) of the energy growth depends on the directionality of the existing spectrum. However many models, including the SOWM, employ a point spectral growth mechanism and spread the energy growth over direction with a spreading function. This is done presumably due to the lack of a form of the atmospheric energy input as a function of the angle between wind and wave.

In this study, such a function is developed and employed in a fully directional wave growth mechanism. A discrete spectral model using this growth mechanism is assembled following the operation of the SOWM. The performance of this new model under several sets of conditions is compared with that of a version of the SOWM written by the authors.

2. Structure of the Model

The rate of change of the wave spectrum can be described by the energy balance equation proposed by Hasselmann (1960)

$$\frac{\partial E(f, \theta; \vec{x}, t)}{\partial t} + \vec{C}_g \cdot \nabla E(f, \theta; \vec{x}, t) = S(f, \theta; \vec{x}, t) = S_{in} + S_{nl} - S_{ds} \quad (1)$$

where $E(f, \theta; \vec{x}, t)$ is the two-dimensional directional frequency wave spectrum being a function of position \vec{x} , time t , wave frequency f , and direction of propagation θ . \vec{C}_g is the group velocity of the spectral component and S represents the sum of individual source functions. S_{in} , S_{nl} , and S_{ds} represent the wind input, nonlinear wave interaction and dissipation source functions respectively. As in the SOWM, nonlinear wave interaction is not explicitly modeled. It is generally accepted that the nonlinear interaction is important for wave growth (SWAMP Group, 1985).

The energy input from the wind S_{in} is represented as

$$S_{in} = A(u, f, \alpha) + B(u^*, f, \alpha)E(f, \theta; \vec{x}, t) \quad (2)$$

where u is the wind velocity, u^* is the friction velocity and α is the angle between the wind and wave directions. The A term represents energy transfer from the turbulent pressure fluctuations to the wave field according to the theory of Phillips (1957) and results in a linear growth of the spectrum. The BE term represents the interaction of an already disturbed surface with the wind.

If we consider an infinite ocean with a homogeneous wind field, the wave spectrum is not a function of position. The numerical model for this case requires only one spacial grid point and no propagation scheme. Without the nonlinear interaction and dissipation terms, equation (1) then becomes

$$\frac{\partial E(f, \theta; t)}{\partial t} = A(u, f, \alpha) + B(u^*, f, \alpha)E(f, \theta; t) \quad (3)$$

Since equation (3) is linear, each spectral component can grow independently. Also, according to equation (3) the spectral component can grow to an infinite value with time, but in the real situation, dissipation will limit the growth. Wave breaking is thought to be the main mechanism of dissipation. The dissipation function S_{ds} is applied implicitly for wave energy propagating within $\pm 90^\circ$ of the wind direction in a manner analogous to its implementation in the SOWM. The growth of the spectrum is limited by a fully developed spectrum which will be discussed later.

The directional treatment of the wave growth mechanism is the focus of this study. Before we refer to our model, it is helpful to examine the relation of the energy balance used in the SOWM to equation (3). A directional spectrum can be obtained by multiplying the frequency spectrum by a spreading function:

$$E(f, \theta) = E(f)F(\theta) \quad (4)$$

The spreading function used in the SOWM is that which was derived by the SWOP project (Cote, et al., 1960). It was considered to be a function of wind speed and frequency as well as direction and is given by

$$F(\omega, \alpha, u) = \frac{1}{\pi} \left[1 + (0.5 + 0.82e^{-1/2(\frac{\omega u}{g})^4}) \cos 2\alpha + 0.32e^{-1/2(\frac{\omega u}{g})^4} \cos 4\alpha \right]$$

$$\text{for } -\frac{\pi}{2} < \alpha < \frac{\pi}{2} \quad (5)$$

where $\omega = 2\pi f$ and $F(\omega, \alpha, u) = 0$, elsewhere.

Using equation (4), equation (3) can be rewritten as

$$\frac{\partial E(f; t) F(\alpha)}{\partial t} = A(u, f, \alpha) + B(u^*, f, \alpha) E(f; t) F(\alpha) \quad (6)$$

Integrating equation (6) over the parameter α from $-\pi/2$ to $\pi/2$,

$$\int_{-\pi/2}^{+\pi/2} \frac{\partial E(f; t) F(\alpha)}{\partial t} d\alpha = \int_{-\pi/2}^{+\pi/2} A(u, f, \alpha) d\alpha + \int_{-\pi/2}^{+\pi/2} B(u^*, f, \alpha) E(f; t) F(\alpha) d\alpha \quad (7)$$

If we let

$$A'(u, f) = \int_{-\pi/2}^{+\pi/2} A(u, f, \alpha) d\alpha \quad (8)$$

$$B'(u, f) = \int_{-\pi/2}^{+\pi/2} B(u^*, f, \alpha) F(\alpha) d\alpha \quad (9)$$

and consider that

$$\int_{-\pi/2}^{+\pi/2} F(\theta) d\theta = 1 \quad (10)$$

then we have

$$\frac{\partial E(f; t)}{\partial t} = A'(u, f) + B'(u^*, f) E(f) \quad (11)$$

This directionally integrated energy balance equation, modified to limit spectral values to a fully developed limit, is what is used by

the SOWM. Notice that it assumes that the spectrum is always centered on the wind direction, although the SOWM does not constrain it to be. The directional spectrum is obtained by spreading the growth resulting from this directionally integrated equation at each time step about the wind direction and adding it to the pre-existing directional spectrum, thus forcing the new spectral growth to have the angular distribution of the spreading function.

The model presented in this study solves the energy balance equation in the directional form, equation (3). It does not require the introduction of the artificial angular spreading function and it retains the directionality of the growth. Note that the spectral growth rate is highly dependent on the spectral value through the BE term. The directionality (and magnitude) of the growth will thus depend on the directional properties of the spectrum. This dependence is destroyed if the growth is obtained from equation (11).

3. The A Term

The A(u,f,α) term represents the generation of waves on an initially calm water surface through the turbulent atmospheric pressure fluctuations. It is too weak to explain the major growth of the wave field but it can explain the growth of waves from initially calm water to a certain level where other mechanisms become dominant. Within Phillips' theory, the waves develop most rapidly by means of a resonance mechanism which occurs when a component of the surface pressure distribution moves at the same speed as the free surface wave with the same wave number.

The form of the A function used here is similar to that used by Barnett (1968) and is simply a nonintegrated form of the function used in the SOWM. A summary of the mathematical background is as follows.

Hasselmann (1960) has shown that the A function can be represented in terms of the three-dimensional spectrum of the random atmospheric pressure fluctuations $\Pi(\vec{k}, \omega)$. That is

$$A = \frac{4\pi^2 k \omega^3}{\rho_w g^3} \Pi(\vec{k}, \omega) \tag{12}$$

where k is the magnitude of the wave number $\vec{k} = (k_1, k_2)$, and ρ_w is the density of sea water. From the experiments of Priestly (1965) and discussion of Snyder and Cox (1966), we find

$$\Pi(\vec{k}, \omega) = \frac{1.23A^*}{\pi^2 \omega^2} u^* \frac{0.33k^{1.28}}{0.1089k^{2.56} + (k \cos \alpha - \kappa)^2} \cdot \frac{0.52k^{0.95}}{0.2704k^{1.9} + k^2 \sin^2 \alpha} \tag{13}$$

where κ is ω/u_c , u_c being the convection velocity of the eddies. The value of the coefficient A^* is determined from the measurements of Snyder and Cox with additional data supplied by Cardone (1969). Since this data was related to the wind velocity at 6.1 m above the sea surface the convection velocity is taken as $u_{6.1}$. Priestly's measurements indicate a modification is appropriate for $\kappa < 0.02$. The form of the A function is then

$$A(f, u_{6.1}, \alpha) = \frac{4.793 \times 10^{-16} \omega^4 u_{6.1}^3}{Q_1(\omega, u_{6.1}, \alpha) R_1(\omega, u_{6.1}, \alpha)} \quad \frac{\omega}{u_{6.1}} \leq 0.02 \quad (14)$$

$$A(f, u_{6.1}, \alpha) = \frac{7.167 \times 10^{-14} \omega^{5.25} u_{6.1}^{1.75}}{Q_2(\omega, u_{6.1}, \alpha) R_2(\omega, u_{6.1}, \alpha)} \quad \frac{\omega}{u_{6.1}} > 0.02 \quad (15)$$

and

$$Q_1 = Q_2 = 0.2704 \left(\frac{\omega}{u_{6.1}} \right)^2 + \left(\frac{\omega^2}{g} \sin \alpha \right)^2 \quad (16)$$

$$R_1 = 4.87 \times 10^{-6} + \left(\frac{\omega^2}{g} \cos \alpha - \frac{\omega}{u_{6.1}} \right)^2 \quad (17)$$

$$R_2 = 0.1089 \left(\frac{\omega^2}{g} \right)^{2.5} + \left(\frac{\omega^2}{g} \cos \alpha - \frac{\omega}{u_{6.1}} \right)^2 \quad (18)$$

A is in m^2/rad , $u_{6.1}$ is in m/sec , and g is in m/sec^2 .

It should be noted that the numerical constants appearing in equation (14) and (15) are not those given in Pierson (1982). He gives the form of A used in the computer code where for computational convenience it has been multiplied by the minimum frequency bandwidth (1/180 sec) and the number of seconds in his 3 hour time step. His value for A is also off by a factor of two which was applied separately in the SOWM code.

4. The BE Term

The $B(u, f, \alpha)E(f, \theta; t)$ term is the result of the interaction of the air flow with the already disturbed water surface. Miles (1957) considered the perturbation of the mean shear flow in the air by the disturbed water surface, but he neglected the effects of atmospheric turbulence. Phillips (1966) extended the analysis to consider the interaction of the wave induced air flow perturbations with the free stream turbulence. He derived an expression in terms of the mean velocity profile of the wind, U , as follows

$$\frac{B}{f} = \frac{\rho_a}{\rho_w} \frac{1}{c^2 k} \left\{ \frac{M_m N^2 k^4}{\cos^2 \alpha} \left(\frac{-U'''}{(U')^3} \right) z_m \left(\int_{z_m}^{\infty} [U(z) \cos \alpha - c]^2 e^{-kz} dz \right)^2 \right. \\ \left. + M \int_0^{\infty} N^2 (-U''') \cos \alpha |U \cos \alpha - c| e^{-2kz} dz \right\} \quad (19)$$

where M , M_m and N are constants and z_m is the matched height where the mean wind speed, $U(z_m)$, is equal to the wave phase speed, c . Phillips suggested $M_m = \pi$, $M = 1.6 \times 10^{-2}$, $N^2 = \frac{1}{3}$ for $z > z_m$ and $N^2 = 1$ for $z < z_m$. Inoue (1967) used these values and assumed a logarithmic velocity profile to evaluate equation (19). He found poor agreement with observational data and abandoned this approach. For his B function he fit a curve to data obtained from wave growth measurements. The function he found and that which is used in the SOWM is

$$\frac{B}{f} = 0.00139 e^{-7.0000 \left[\left(\frac{u}{c} \right)^* - 0.031 \right]^2} + 0.725 \left(\frac{u}{c} \right)^* e^{-0.00004 \left(\frac{u}{u^*} \right)^2} \quad (20)$$

We repeated the calculations of Inoue (1967) using a logarithmic velocity profile in equation (19) and found directionally integrated results much larger than given by equation (20). Looking at the integrand of the second term in (19), we found that it became very large for small z since the logarithmic profile has a very large curvature near the surface. Note that the lower limit of this integration is actually the roughness height, z_0 , for the logarithmic profile. From these calculations, it appears that the mean velocity must have much less curvature near the surface than is given by the logarithmic profile. Takeda (1963) has measured departures from a logarithmic form very close to the water surface.

In this study, rather than attempting to derive a more appropriate mean velocity profile, Gauss-Laguerre quadrature is used in an effort to avoid the contribution to the integration from this strong peak near the origin. Thus we are integrating a polynomial fit to the integrand which does not follow the peak. In effect, we are assuming a

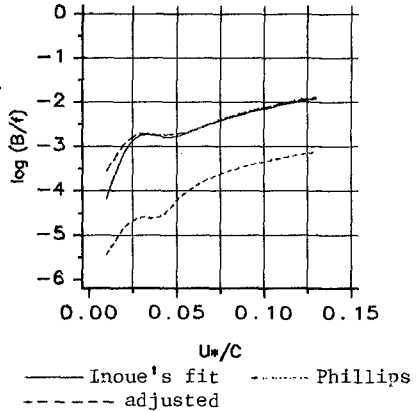


Fig. 1. Evaluation of the B function in directionally integrated form

mean velocity profile which would give us the integrand matching this polynomial fit. The result of evaluating equation (19) in this manner, using the values of the constants suggested by Phillips, and integrating over direction according to equation (9) is shown as the lowest curve in Figure 1. The solid line in this figure is Inoue's curve fit to the observational data, equation (20). The constants M and M_m in equation (19) were adjusted to give agreement with it, requiring the values 1.2 and 12π , respectively. The result using these constants is the remaining curve in Figure 1.

5. Other Details of the Model

As does the SOWM, our model does not explicitly model the dissipation for waves traveling with the wind. A limiting directional wave spectrum is assumed as a function of wind speed. The form used here (and in the SOWM) is the Pierson-Moskowitz spectrum, $E_{\infty}(\omega, u)$, with the directionality of the SWOP spreading function. The fully developed spectrum is thus

$$E_{\infty}(\omega, \alpha, u) = E_{\infty}(\omega, u)F(\omega, \alpha, u) \quad (21)$$

Following Inoue (1967), energy dissipation is assumed to be a function of the ratio of the spectrum to the fully developed spectrum. Then equation (3) can be written as

$$\begin{aligned} \frac{\partial E(f, \theta; t)}{\partial t} = & A(u, f, \alpha) + B(u^*, f, \alpha)E(f, \theta; t) \\ & - [A(u, f, \alpha) + B(u^*, f, \alpha)E(f, \theta; t)] \left[\frac{E(f, \theta; t)}{E_{\infty}(f, \alpha, u)} \right]^2 \end{aligned} \quad (22)$$

A closed form solution may be obtained if we multiply A by $[1 - (\frac{E}{E_{\infty}})^2]^{1/2}$. This has only a small effect on the growth of the spectrum. Equation (23) can then be written as

$$\frac{dE}{dt} = \{A[1 - (\frac{E}{E_{\infty}})^2]^{1/2} + BE\} [1 - (\frac{E}{E_{\infty}})^2] \quad (23)$$

with solution

$$E = \frac{A[e^{Bt} - 1]}{B} \left\{ 1 + \left[\frac{A(e^{Bt} - 1)}{BE_{\infty}} \right]^2 \right\}^{-1/2} \quad (24)$$

Equation (24) is applied in a directional form in a manner analogous to its directionally integrated application in the SOWM. At each time step, each frequency-direction band that lies within $\pm 90^\circ$ to the wind direction is allowed to grow if its initial value is less than $0.95E_{\infty}(f, \theta)$. If $0.95E_{\infty} \leq E < E_{\infty}$, E is set equal to its fully developed

value. If the initial value exceeds E_{∞} , no growth is allowed. Thus under a steady wind, each component will grow until it reaches its fully developed limit. Once all bands have reached saturation, the spectrum reaches a steady state.

If the wind now turns, since the fully developed spectrum is tied to the wind direction, some bands (within $\pm 90^\circ$ to the wind direction) will exceed their fully developed limit while others will not. If these underdeveloped bands are allowed to grow, the total energy present will exceed that in our fully developed sea. This situation also arises in the SOWM but is given special treatment here. We allow normal growth in those direction bands less than fully developed and attenuate the energy in over developed bands to maintain the same total energy in each frequency band.

Waves traveling at angles greater than $\pm 90^\circ$ to the wind direction are explicitly dissipated in the same manner as is done in the SOWM. The rate of dissipation depends on the total energy traveling within $\pm 90^\circ$ to the wind direction and the relative angle between wind and wave. The expression used is

$$E_d(f, \theta, t) = E_o(f, \theta, t) \left[e^{-s \Delta t (E_e(t))^{1/2} f^4} \right] r(\theta) \quad (25)$$

where E_d is the spectral component after dissipation. E_o is the spectral component before dissipation, E_e is the total energy of the wind sea traveling within $\pm 90^\circ$ to the wind direction. And where $r(\theta) = 0$ for $\theta \leq 90^\circ$, $\theta \geq 270^\circ$. $r(\theta) = 3$ for $90^\circ < \theta \leq 135^\circ$, $225^\circ \leq \theta < 270^\circ$. $r(\theta) = 4.5$ for $135^\circ < \theta \leq 165^\circ$, $195^\circ \leq \theta < 225^\circ$. $r(\theta) = 6$ for $165^\circ < \theta < 195^\circ$. $s = 754.6 \left(\frac{\text{sec}^4}{\text{m}} \right)$ and Δt is the time step in hours.

As mentioned in the introduction, two model codes were written. One using the formulation of the SOWM code and one, the directional formulation described above. In the following, the former is referred to as VSOWM while the latter is called VPINK. Both models use 53 frequency bands, each of width 0.005 Hz, from 0.04 Hz to 0.3 Hz and 36 directional bands each 10° wide. In a test of CPU time necessary to complete 14 time steps with the infinite ocean models, VPINK required 2.3 times the time needed to run VSOWM.

6. Computational Results and Discussion

All computations were performed with wind speed at 19.5 m of 40 knots (20.6 m/s) and a time step of three hours. The results are presented in both point spectral form and in polar contour plots of the directional spectra. The point spectra include a dashed curve. This is the Pierson-Moskowitz spectrum which is our fully developed spectrum. The contour plots include an arrow which indicates the wind direction. Contours are drawn at increments of 10% of the maximum spectral value present in each plot.

The first case presented is that of wave growth on an initially calm sea under the influence of a steady wind. Figure 2 shows the evaluation of the frequency spectrum from VSOWM and Figure 3 is the same from VPINK. The VPINK spectra are similar to the VSOWM spectra except that the growth slows as a frequency band approaches the fully developed

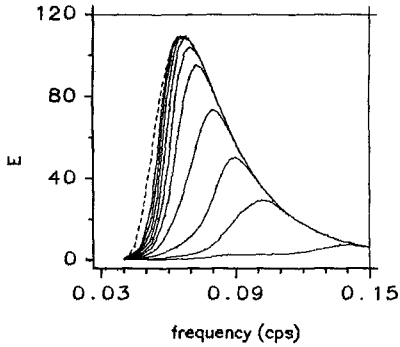


Fig. 2. Point spectrum evolution for a steady wind from VSOWM.

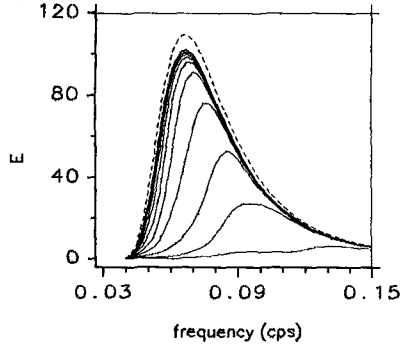


Fig. 3. Point spectrum evolution for a steady wind from VPINK.

limit. The reason for this is that its directional spread is more narrow than the spreading function which we use to define our directional fully developed limit. The direction bands near the wind direction therefore reach saturation first and the more oblique bands continue to grow slowly to fill in the frequency spectrum. This can be seen in the directional spectra of Figures 4 and 5. They are after five time steps from the VSOWM and VPINK respectively. Figure 4, the VSOWM spectrum,

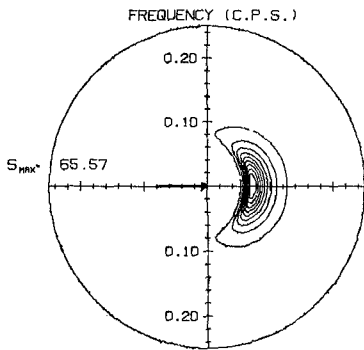


Fig. 4. Directional spectrum at 15 hours from VSOWM - steady wind.

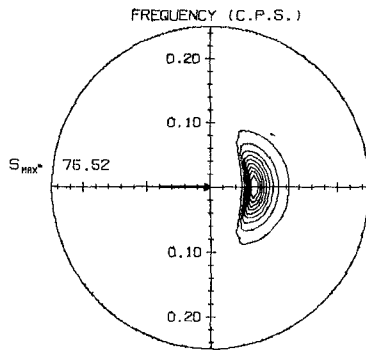


Fig. 5. Directional spectrum at 15 hours from VPINK - steady wind.

has the directionality of the spreading function while the VPINK spectrum in Figure 5 has a narrower spread which was determined by the growth mechanism. The difference in significant wave heights vs. time is small.

For the next case the sea was initially calm and the wind direction was allowed to vary by 10° at each time step, sweeping back and forth between $\pm 20^\circ$. This demonstrated two points. First, the frequency spectra agreed more closely; each resembled the VSOWM steady wind case. This suggests that the typical fluctuations of wind direction may have a significant impact on the wave field directionality. The second point is that once the wave energy present within $\pm 90^\circ$ to the wind direction at a given frequency reaches its saturation level, the evolution of the VSOWM spectrum ceases whereas the directional relaxation mechanism previously discussed becomes active in VPINK. The VSOWM spectrum "freezes" from higher to lower frequencies as each reaches saturation while the VPINK spectrum continues to follow the wind vector (with some time lag). Typical directional spectra are shown in Figures 6 and 7.

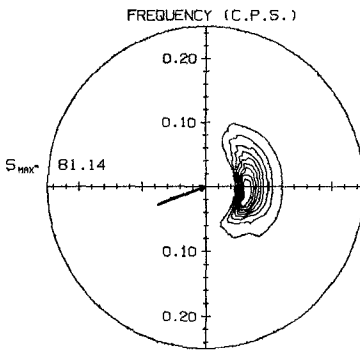


Fig. 6. Directional spectrum at 33 hours from VSOWM - oscillating wind.

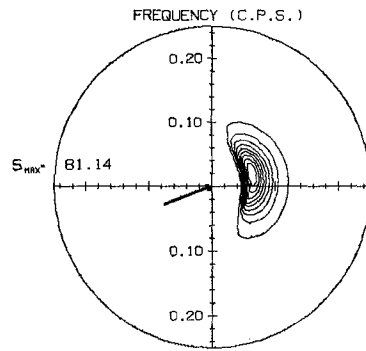


Fig. 7. Directional spectrum at 33 hours from VPINK - oscillating wind.

In the VSOWM spectrum of Figure 6, only those frequencies well below the modal frequency respond to the changing wind direction, quite the opposite of what we would expect to occur naturally. The VPINK spectrum in Figure 7 retains its response to the changing wind direction.

This same problem with VSOWM has even greater consequences when we consider a sudden 90° change of wind direction. We start with a fully developed sea spread about 90° and at $t = 0$ the wind direction changes to 0° . The VSOWM spectrum soon freezes up in a bidirectional form. The wave energy initially travelling in directions $0^\circ < \theta < 90^\circ$ is unchanged, new energy spread about the wind direction quickly grows to saturate each frequency band and thereafter, the only change is the attenuation of the energy initially in the directions $90^\circ < \theta < 180^\circ$. The directional spectrum at $t = 30$ hours is shown in Figure 8. The

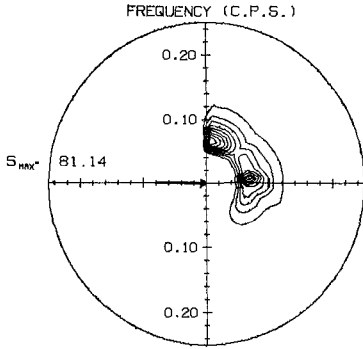


Fig. 8. Directional spectrum at 30 hours from VSOWM - 90° wind direction change.

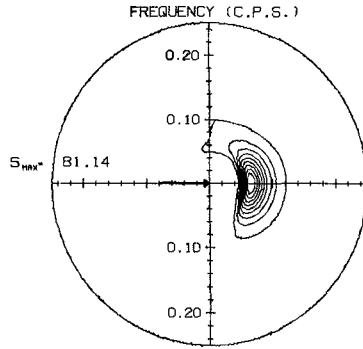


Fig. 9. Directional spectrum at 30 hours from VPINK - 90° wind direction change.

corresponding VPINK spectrum is shown in Figure 9. It evolves more naturally with the gradual growth of waves in the new direction and decay of the other components.

The final, and perhaps most important, comparison case does not involve a freezing up but addresses the fundamental nature of the point spectral growth mechanism. In this case we leave the wind steady but start with an initial low frequency swell on an otherwise calm sea. VPINK is little affected by the swell as can be seen by the point spectral evolution in Figure 10. Directional spectra at $t = 3, 9$ and 15

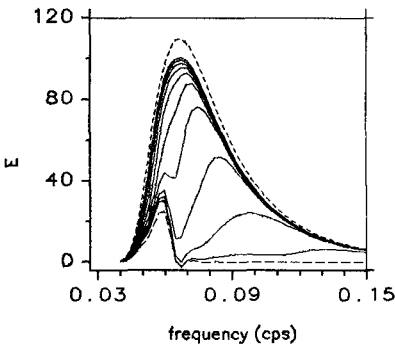


Fig. 10. Point spectrum evolution in the presence of swell from VPINK.

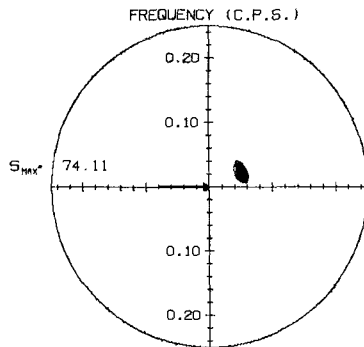


Fig. 11. Directional spectrum at 3 hours from VPINK - initial swell case.

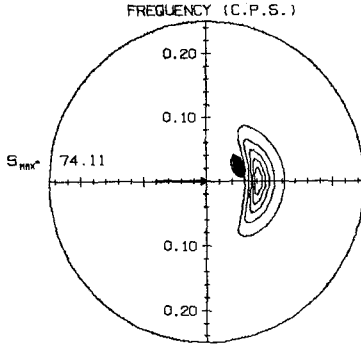


Fig. 12. Directional spectrum at 9 hours from VPINK - initial swell case.

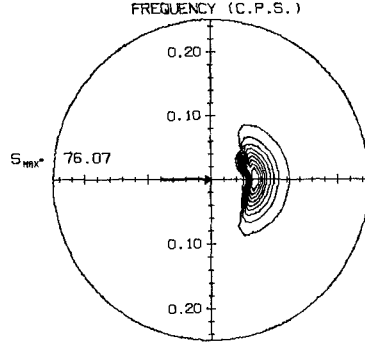


Fig. 13. Directional spectrum at 15 hours from VPINK - initial swell case.

hours are shown in Figures 11, 12 and 13 respectively. Figure 11 is nearly identical to the initial condition. As time proceeds, the wind sea grows to envelope the swell. The point spectral growth mechanism of the VSOWM however assumes that the initial energy present is centered on the wind direction and produces a much larger amount of growth in these frequency bands as can be seen in Figure 14. Figures 15, 16 and 17 are

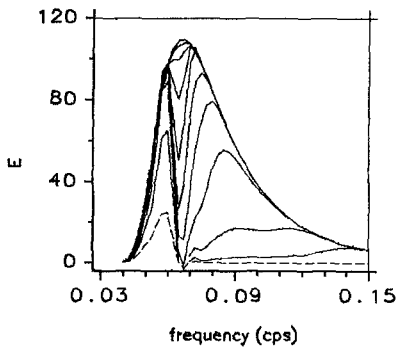


Fig. 14. Point spectrum evolution in the presence of swell from VSOWM.

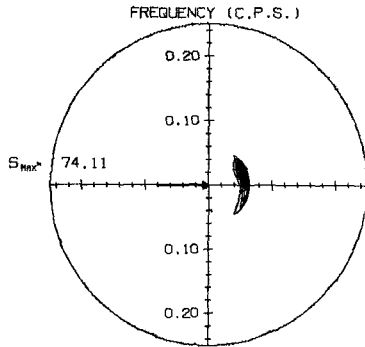


Fig. 15. Directional spectrum at 3 hours from VSOWM - initial swell case.

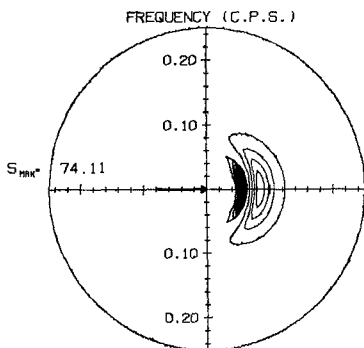


Fig. 16. Directional spectrum at 9 hours from VSOWM - initial swell case.

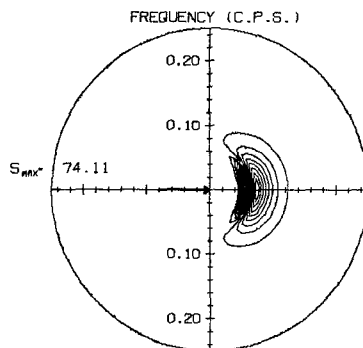


Fig. 17. Directional spectrum at 15 hours from VSOWM - initial swell case.

the directional spectra for $t = 3, 9,$ and 15 hours respectively from VSOWM. From these we see that this new energy is spread widely in direction creating new low frequency components that should take much longer to develop.

These strong low frequency components, spread over $\pm 90^\circ$ are created due to a swell initially very narrowly spread. If this behavior is coupled with a propagation scheme, as it is in the operational SOWM, and these components are propagated to adjacent grid points, at those points they will act similar to the initial swell here. It is not hard to see that this growth mechanism could quickly corrupt a large area with excess low frequency energy, carried predominantly in the wind direction. Lazanoff and Stevenson (1975) describe several high energy case studies made for verification of the SOWM. Among the inaccuracies noted were the propagation of wave energy in improper directions and frequency shifts of spectral peaks. The problems discussed here may very well be responsible for these discrepancies. It also seems likely that the twenty year hindcast wave climatology produced with the SOWM (Lee, Bales and Sowby, 1985) overestimates both the low frequency wave energy present and its directional spread.

Acknowledgement

This work was supported by the David Taylor Naval Ship Research and Development Center under P.E. 62759N, SF-59-557-695.

References

- Barnett, T.P. (1968): On the generation, dissipation, and prediction of ocean wind waves. *J. Geophys. Res.* 73, 513-529.
- Cardone, V.J. (1969): Specification of the wind distribution in the marine boundary layer for wave forecasting. New York University, Department of Meteorology and Oceanography, TR 69-1, 11 pp.

- Cote, L.J., J.O. Davis, W. Marks, R.J. McGough, E. Mehr, W.J. Pierson, Jr., F.J. Ropek, G. Stephenson and R.C. Vetter (1960): The directional spectrum of a wind generated sea as determined from data obtained by the Stereo Wave Observation Project. Meteor. Pap., Vol. 2, No. 6, 88 pp., New York University Press, NY.
- Ewing, J.A. (1971): A numerical wave prediction method for the North Atlantic Ocean: Dtsch. Hydrogr. Z. 24, 241-261.
- Golding, B. (1983): A wave prediction system for real-time sea state forecasting. Quart. J.R. Met. Soc., 109, 393-416.
- Hasselmann, K. (1960): Grundgleichungen der Seegangsveroussage. Schiffstechnik, 7, 191.
- Hasselmann, K., T.P. Barnett, E. Bouws, H. Carlson, D.E. Cartwright, K. Enke, J.A. Ewing, H. Grenopp, D.G. Hasselmann, P. Kruesman, A. Meerburg, P. Muller, D.J. Olbers, K. Richter, W. Sell and H. Walden (1973): Measurements of wind wave growth and swell decay during the joint North Sea Wave Project (JONSWAP). Dtsch. Hydrogr. Z., Suppl. A. 8(12).
- Hasselmann, K., D.B. Ross, P. Muller and W. Sell (1976): A parametrical wave prediction model. J. Phys. Oceanogr., 6, 200-228.
- Inoue, T. (1967): On the growth of the spectrum of a wind generated sea according to a modified Miles-Phillips mechanism and its application to wave forecasting. TR-67-5, Geophysical Science Laboratory Report, NY University, School of Engineering and Science.
- Lazanoff, S.M. and N.M. Stevenson (1975): An evaluation of a hemispheric operational wave spectral model. Tech. Note 75-3, Fleet Numerical Weather Center, Monterey, CA.
- Lee, W.T., S.L. Bales and S.E. Sowby (1985): Standardized wind and wave environments for North Pacific Ocean Areas. DTNSRDC/SPO-0919-02.
- Miles, J.W. (1957): On the generation of surface waves by shear flow, Part 1, J. Fluid Mech., 185-204.
- Phillips, O.M. (1957): On the generation of surface waves by turbulent wind, J. Fluid Mech., 2, 417-445.
- Phillips, O.M. (1966): The dynamics of the upper ocean. Cambridge University Press, NY.
- Pierson, W.J., L. Tick and L. Baer (1966): Computer based procedures for preparing global wave forecasts and wind field analyses capable of using wave data obtained by a space craft. Proc. 6th Naval Hydrodynamics Symp., Vol. 2, 1.
- Pierson, W.J. (1982): The spectral ocean wave model (SOWM), A northern hemisphere computer model for specifying and forecasting ocean wave spectra. DTNSRDC-82/011.
- Priestly, J.T. (1965): Correlation studies of pressure fluctuations on the ground beneath a turbulent boundary layer. Natl. Bur. Std. Rpt. 8942.
- Resio, D.T. (1981): The estimation of wind-wave generation in a discrete spectral model. J. Geophys. Oceanogr., 11, 510-525.
- Snyder, O.H. and C.S. Cox (1966): A field study of the wind generation in a discrete spectral model for specifying and forecasting ocean wave. J. Marine Res., 24(2), 141-178.
- SWAMP group (1985): Ocean wave modeling. Plenum Press, NY and London.
- Takeda, A. (1963): Wind profiles over sea waves. J. Ocean. Soc., Japan, 19, 16-22.